

## Research Article

# Characteristics of UV-MicroO<sub>3</sub> Reactor and Its Application to Microcystins Degradation during Surface Water Treatment

Guangcan Zhu, Xiwu Lu, and Zhonglian Yang

School of Energy and Environment, Key Laboratory of Environmental Medicine Engineering, Ministry of Education, Southeast University, Nanjing 210096, China

Correspondence should be addressed to Guangcan Zhu; gc-zhu@seu.edu.cn

Received 22 February 2015; Accepted 31 March 2015

Academic Editor: Jian Lu

Copyright © 2015 Guangcan Zhu et al. This is an open access article distributed under the Creative Commons Attribution License, which permits unrestricted use, distribution, and reproduction in any medium, provided the original work is properly cited.

The UV-ozone (UV-O<sub>3</sub>) process is not widely applied in wastewater and potable water treatment partly for the relatively high cost since complicated UV radiation and ozone generating systems are utilized. The UV-microozone (UV-microO<sub>3</sub>), a new advanced process that can solve the abovementioned problems, was introduced in this study. The effects of air flux, air pressure, and air humidity on generation and concentration of O<sub>3</sub> in UV-microO<sub>3</sub> reactor were investigated. The utilization of this UV-microO<sub>3</sub> reactor in microcystins (MCs) degradation was also carried out. Experimental results indicated that the optimum air flux in the reactor equipped with 37 mm diameter quartz tube was determined to be 18~25 L/h for efficient O<sub>3</sub> generation. The air pressure and humidity in UV-microO<sub>3</sub> reactor should be low enough in order to get optimum O<sub>3</sub> output. Moreover, microcystin-RR, YR, and LR (MC-RR, MC-YR, and MC-LR) could be degraded effectively by UV-microO<sub>3</sub> process. The degradation of different MCs was characterized by first-order reaction kinetics. The pseudofirst-order kinetic constants for MC-RR, MC-YR, and MC-LR degradation were 0.0093, 0.0215, and 0.0286 min<sup>-1</sup>, respectively. Glucose had no influence on MC degradation through UV-microO<sub>3</sub>. The UV-microO<sub>3</sub> process is hence recommended as a suitable advanced treatment method for dissolved MCs degradation.

## 1. Introduction

As a combination of ozonation and photochemical excitation, the ultraviolet-ozone (UV-O<sub>3</sub>) process is based on the effect of hydroxyl radical (<sup>•</sup>OH) generated from UV radiation and ozone photolysis to improve the oxidation capability [1, 2]. It has been known that <sup>•</sup>OH reacts very quickly with many organic species, displaying kinetic constants in the range of 10<sup>8</sup> to 10<sup>10</sup> M<sup>-1</sup> s<sup>-1</sup> [3]. Previous studies have demonstrated the efficient degradation of various organic compounds such as phenol [4], linuron [5], haloacetic acids [6], and N-nitrosodimethylamine [7], in aqueous solution by the UV-O<sub>3</sub> process. However, the utilization of complicated UV radiation and O<sub>3</sub> generating systems, together with the high energy consumption, leads to relatively high cost which limits the wide application of this process [8]. To solve this problem, a new advanced process, UV-microO<sub>3</sub>, was developed [9]. In a UV-microO<sub>3</sub> reactor, the O<sub>3</sub> concentration is less than 1 mg/L, and it is generated from dry air by UV-radiation with primary emission at 253.7 nm and 185 nm. No ozone

generator is needed in this new process. The study conducted by Zhao et al. [10] showed that the <sup>•</sup>OH radical exposure in UV-microO<sub>3</sub> process was significantly higher than that in UV-air system, and thus UV-microO<sub>3</sub> process could remove aniline more efficiently. The UV systems with internal O<sub>3</sub> generation were also carried out for odour compounds treatment by Kutschera et al. [11] and Zoschke et al. [12]. However, ozone generation in UV-microO<sub>3</sub> process is not mentioned in these above studies, and researches on organic contaminants removal by UV-microO<sub>3</sub> process are still limited.

Microcystins (MCs) are hepatotoxins containing cyclic heptapeptides produced by cyanobacteria. Regarding microcystins, researchers have found more than 80 isomers, in which microcystin-RR, YR, and LR (MC-LR, MC-RR, and MC-YR) are the most important isomers [13]. As a consequence of significant stability in wide pH and temperature ranges, the MCs usually exist in natural water for several days to several weeks [14]. Researches have verified that MCs are also strong promoters to liver tumor [15] since the first investigation that *Nodularia spumigena* can poison

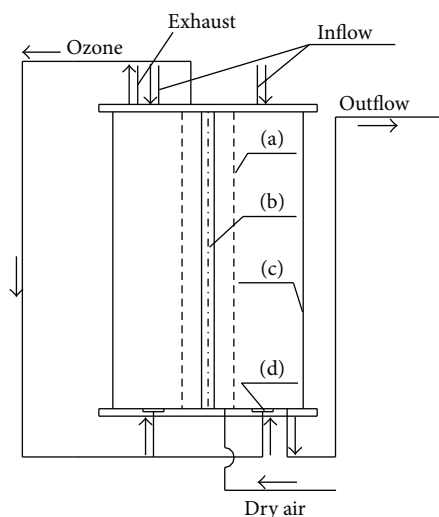


FIGURE 1: Construction of UV-microO<sub>3</sub> Reactor. (a) Quartz tube, (b) UV lamp, (c) glass tube, and (d) microporous titanium plate.

livestocks and birds. Afterwards, it has also been reported that both human beings and animals could be poisoned even to death by drinking the water containing MCs. However, conventional water treatment systems have been proven to be unreliable for the removal of these toxins [16]. Researchers have reported that MCs can be degraded by UV radiation [17] and can be oxidized by O<sub>3</sub> [18]. Other studies have also shown that UV, O<sub>3</sub>, and advanced oxidation processes were effective ways to destroy MCs [19–21]. The influencing factors such as O<sub>3</sub> dose [22–24] and natural organic material (NOM) [25–27] have been examined for the degradation of organic contaminants including MCs. Nevertheless, few researchers have focused on MCs degradation as well as its influencing factors in UV-microO<sub>3</sub> process. And the decomposition mechanism of MCs together with the effects of glucose on MCs degradation in UV-microO<sub>3</sub> process has never been reported.

Therefore, based on these previous studies, this paper introduced the UV-microO<sub>3</sub> process to degrade MCs in water. And the influencing factors of O<sub>3</sub> generation and MCs degradation were also examined in this study. The aim of this research was to determine the optimum parameters for the UV-microO<sub>3</sub> process and to explore the mechanism of this process.

## 2. Materials and Methods

**2.1. Structure and Configuration of UV-MicroO<sub>3</sub> Reactor.** The construction of the UV-microO<sub>3</sub> reactor utilized in this investigation was shown in Figure 1. And Figure 2 listed the detailed schematic diagram of the UV-microO<sub>3</sub> process. Additionally, the operational parameters for the UV-microO<sub>3</sub> reactor were listed in Table 1.

As shown in Figure 2, the air used in this process was supplied by oil-less air pump. Before entering the subsequent reactor, the air should be firstly pretreated with procedure summarized as follows: dried through two columns filled

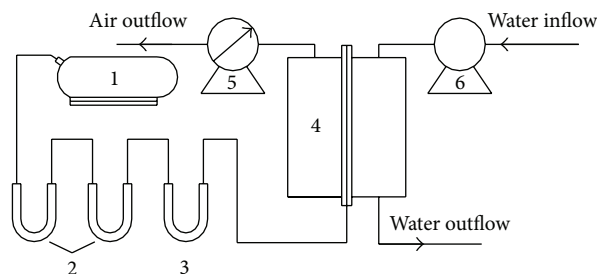


FIGURE 2: Schematic diagram of the UV-microO<sub>3</sub> process. (1) Oil-less air pump, (2) silica gel, (3) fiberglass, (4) photochemical oxidation area, (5) wet type gas flowmeter, and (6) peristaltic pump.

TABLE 1: The operating parameters for the UV-microO<sub>3</sub> reactor.

Parameters	Value
Total diameter × total height, cm × cm	Φ22 × 60
Surface area of microporous titanium plate, cm <sup>2</sup>	7.07
Diameter of microporous titanium plate, μm	1~5
Inner diameter of water tube and air tube, cm	0.4
Inner/external diameter of quartz tube, cm	3.7/4 or 4.4/5.0
Inner/external diameter of reactor, cm	13.6/14.6
Volume, L	4.8
Effective height, cm	41
Sectional area, cm <sup>2</sup>	132.7

with silica gel and filtrated through one column filled with fiberglass. The O<sub>3</sub> gas was generated through UV radiation effect at 253.7 nm. The mixed gas was then introduced into the photochemical oxidation area, in which the raw water was purified by synergistic effect of UV and O<sub>3</sub>.

In order to determine the optimum operational parameters of UV-microO<sub>3</sub> reactor, the effects of air flux, air pressure, and humidity on ozone output and concentration were investigated. In this UV-microO<sub>3</sub> reactor, the air flux rate was adjusted by a flowmeter and the air pressure was adjusted by a valve installed in the end of the air tube. The employed air flow for UV-microO<sub>3</sub> process was comprised by two tributaries, one was dried and filtered and the other was only filtered. Consequently, the humidity of the final air flow could be adjusted by changing the air flow rates of the tributaries.

**2.2. Preparation of Simulated Raw Water Sample.** Cyanobacteria samples were collected at Number 2 Monitor Point of Taihu, when the blue-green algae bloomed. The cyanobacteria samples were concentrated and frozen for subsequent use. The naturally melted samples were shaken intermittently for 30 minutes under ultrasonic wave of 20 MHz in order to destroy the algae cell and release the MCs. The mixed liquid was shaken for 30 minutes again and was then centrifuged for 20 minutes at 5000 rpm, for supernatant collection. These above steps were repeated 3 times to obtain more soluble samples from the solid materials remaining at the cuvette bottom. The liquid product collected three times was mixed

TABLE 2: The characteristics of raw water quality.

Item	COD <sub>Mn</sub> (mg/L) <sup>1,2</sup>	UV <sub>254</sub> (cm <sup>-1</sup> ) <sup>2</sup>	MC-RR (μg/L)	MC-YR (μg/L)	MC-LR (μg/L)
Treated lake water (1#)	2.54	0.156	6.8	3.65	3.41
Pure water with glucose (2#)	2.87	0.073	5.7	2.65	2.3
Pure water (3#)	0	0.073	5.7	2.65	2.3

<sup>1</sup>COD<sub>Mn</sub> was the value without cyanobacteria distillation. <sup>2</sup>Deionized water acted as the reference sample when COD<sub>Mn</sub> or UV<sub>254</sub> was detected.

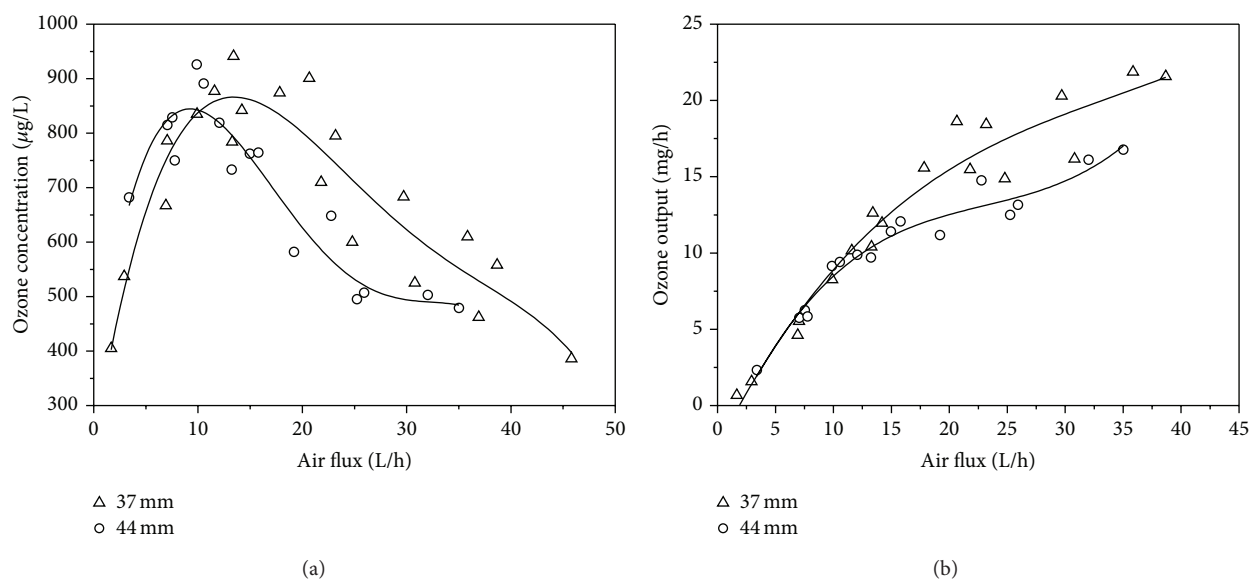


FIGURE 3: Effect of air flux on concentration (a) and ozone output (b).

and then filtrated through 0.45 μm GF/C fiberglass film to obtain the crude extraction.

For the research of microcystin degradation by UV-microO<sub>3</sub> reactor, some of the crude extraction was put into the deionized water to create the simulated raw water sample. For the investigation of organic substance on MC removal, equivalent amounts of cyanobacteria extractions were added into three water samples including deionized water, deionized water containing glucose, and the treated lake water (coagulation, sedimentation, and filtration). The characteristics of raw water quality were listed in Table 2.

**2.3. Microcystin Degradation by UV-MicroO<sub>3</sub> Reactor.** The degradation experiment began after filling 4.5 L raw water sample into the UV-microO<sub>3</sub> reactor. Based on the batch experiment, the MC concentration was separately recorded with time. In the reactor, the air flux, air pressure, and air dew-point temperature varied in the range of 2~47 L/h, 2~19 kPa, and 0~26°C, respectively.

**2.4. Analytical Methods.** High Performance Liquid Chromatography (HPLC, Agilent 1100, Agilent, USA) analysis was used for the determination and measurement of MC-RR, MC-YR, and MC-LR [28]. In the gas phase, O<sub>3</sub> concentration was measured in the gas stream iodometrically by bubbling the gas in a potassium iodide solution. The humidity of inlet

air flow was measured with an air humidity indicator (testo-610, Testo, Germany). Regarding the treatment performance of UV-microO<sub>3</sub> reactor, the water sample after purification was collected to measure the UV<sub>254</sub> absorbance at 254 nm by a UV/Vis spectrophotometer (UV 9100 B, Beijing LabTech Co., Ltd., China) and to detect the COD<sub>Mn</sub> concentration according to the standard methods (APHA, 1995).

### 3. Results and Discussion

**3.1. Effect of Air Flux on O<sub>3</sub> Output and Concentration.** The UV-microO<sub>3</sub> reactor was equipped with two quartz tubes, one with 44 mm diameter and the other with 37 mm diameter. The output and concentration of O<sub>3</sub> gas were measured under various air fluxes, with corresponding results shown in Figure 3.

It was clear from Figure 3 that the discipline for ozone generation along with air flux variation was similar for two reactors with 44 mm and 37 mm diameter. The concentration and output of O<sub>3</sub> showed a markedly increased trend at lower air fluxes. The maximum O<sub>3</sub> concentration was available when the air fluxes were 10 L/h (for quartz tube with 37 mm diameter) and 15 L/h (for quartz tube with 40 mm diameter).

Under the low air flux, the heat from UV lamp could not be transferred to the air in time; therefore, the temperature of the reactor was high, which resulted in the O<sub>3</sub> decomposition. It was believed that with the increase of air flux, temperature

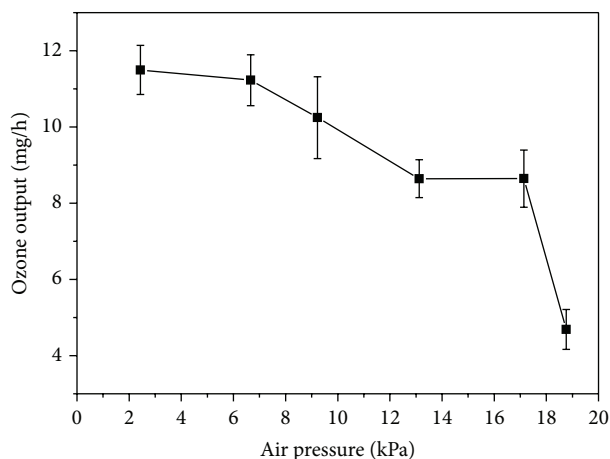


FIGURE 4: Variation of O<sub>3</sub> output under different air pressures.

was not the key factor influencing O<sub>3</sub> output, and the O<sub>3</sub> generation rate was higher than the decomposition rate. When generation rate and decomposition rate came to a dynamic equilibrium, the O<sub>3</sub> concentration reached its maximum. However, further increase of air flux rate did not cause further increase of O<sub>3</sub> concentration (Figure 3) due to the fact that the short residence time was limited the ozone synthesis. It should be noted that, in comparison with the reactor equipped with 37 mm diameter quartz tube, the air in the reactor equipped with 44 mm diameter quartz tube had a longer residence time, so the temperature was correspondingly higher, which led to higher O<sub>3</sub> decomposition rate and lower O<sub>3</sub> output as shown in Figure 3(b).

From the results listed in Figure 3, it was difficult to determine which reactor (37 mm diameter quartz tube or 44 mm diameter quartz tube) was better. Taking the UV-radiation and effective volume into consideration, the reactor equipped with 37 mm diameter quartz tube was selected for further studies. Correspondingly, the optimum air flux of the UV-microO<sub>3</sub> reactor was 18~25 L/h with O<sub>3</sub> generation at a concentration range of 0.67~0.80 mg/L.

**3.2. Effect of Air Pressure on O<sub>3</sub> Output.** The influence of air pressure on output efficiency of O<sub>3</sub> was shown in Figure 4, in which the air pressure varied from 2 kPa to 19 kPa.

The results in Figure 4 showed that, with the increase of air pressure, the O<sub>3</sub> output decreased. It was shown that the high pressure enhanced the collision probability of O<sub>3</sub> molecules, oxygen molecules, oxygen atoms, and reactor walls, which accelerated the O<sub>3</sub> decomposition. In order to get the optimum O<sub>3</sub> output, pressure of the air in UV-microO<sub>3</sub> reactor should be as low as possible. At the same time, the air pressure should also meet the basic demands for O<sub>3</sub> filling and water treatment process.

**3.3. Effect of Air Humidity on O<sub>3</sub> Concentration.** In this section, the experiments were performed in another reactor with height of 890 mm. The power of UV lamp was 30 W and the external diameter of quartz tube was 40 mm. The air flux

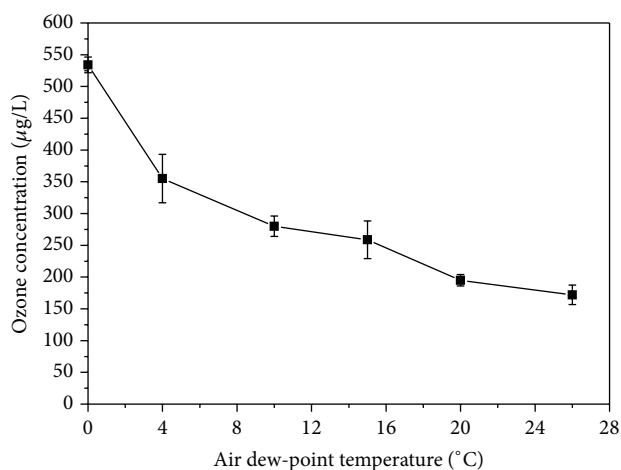
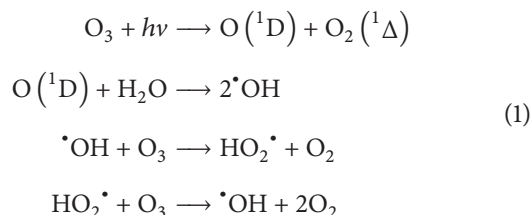


FIGURE 5: Effect of air humidity on ozone concentration.

in the UV-microO<sub>3</sub> was 90 L/h. The results were shown in Figure 5.

From the result shown in Figure 5, it was obvious that O<sub>3</sub> concentration declined when the air dew-point temperature increased at the range of 0~26°C. Under the conditions of UV radiation ( $\lambda = 253.7$  nm), steamed air could enhance the quantum yield of O<sub>3</sub> photodecomposition. The quantum yield increased linearly with the square root of steam partial pressure. The main chain reactions are listed as follows



Consequently, in actual operation, the air humidity in the UV-microO<sub>3</sub> reactor should be reduced as much as possible.

**3.4. Degradation Kinetics of MCs.** Figure 6 listed the variation of MCs concentration along with hydraulic retention time (HRT) and the relationship between MCs content and HRT. It can be seen from Figure 6(a) that MC-RR had the highest concentration within three kinds of MCs investigated in this paper. During the degradation process, the concentration of MCs decreased gradually with the increase of HRT, and the concentrations of MCs tended to be stable after about 90 min.

As shown in Figure 6(b), the degradation of MCs followed pseudofirst-order reaction kinetics. The kinetic equation of MCs degradation was

$$\ln\left(\frac{C}{C_0}\right) = -Kt,
 \tag{2}$$

where  $C$  is MCs concentration in purified water ( $\mu\text{g/L}$ ),  $C_0$  is the concentration of MCs in untreated water ( $\mu\text{g/L}$ ),  $t$  is the reaction time (min), and  $K$  is the reaction rate constant ( $\text{min}^{-1}$ ).

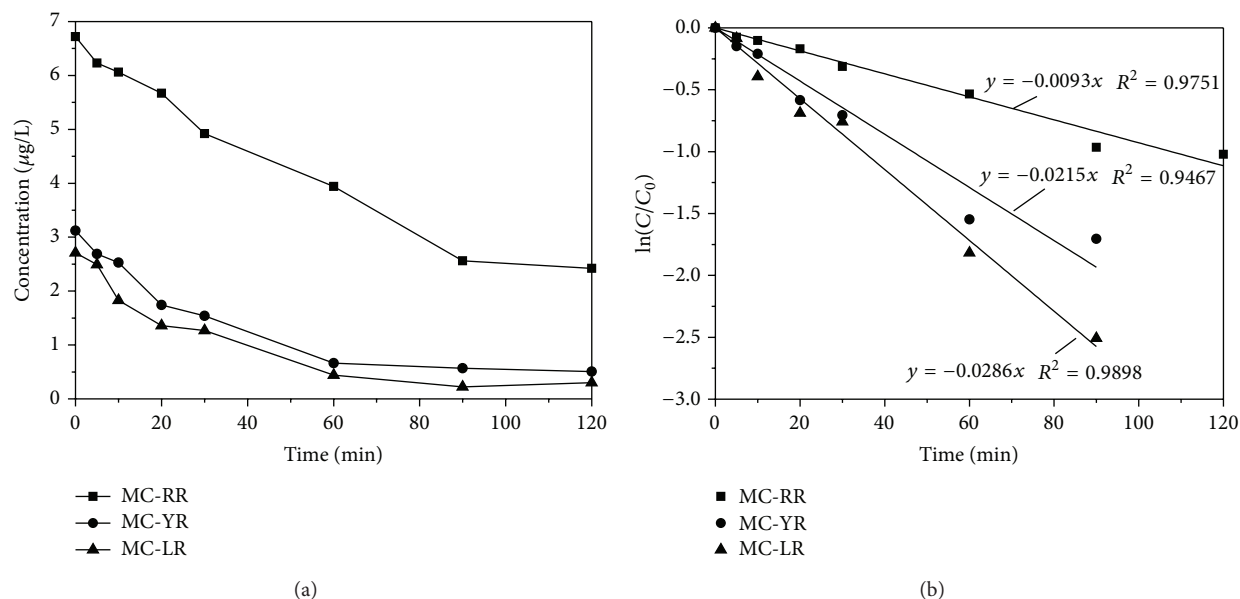


FIGURE 6: Effect of time on the degradation of MCs.

The results showed that the pseudofirst-order kinetic constants ( $K$ ) of MC-RR, MC-YR, and MC-LR degradation were 0.0093, 0.0215, and 0.0286  $\text{min}^{-1}$ , respectively. The half-life times ( $t_{1/2}$ ) for MC-RR, MC-YR, and MC-LR degradation were 74.5, 32.2, and 24.2 minutes, respectively. The degradation rate of MC-LR was a little higher than that of MC-YR. The different reaction rate constants were determined by different molecular structures of MCs. MC-LR had the highest toxicity, but its degradation rate was also the highest. The results have significance for toxin control of MCs in potable water.

The side chain Adda group is the toxic group of MCs [28]. It has conjugated double bond structure [17] which is sensitive to UV radiation. Subsequently, toxicity of MCs can be removed by UV-radiation or hydroxyl radicals through destroying the Adda group [17]. Zhang et al. [29] carried out the MCs degradation by taking 5 mL of cyanobacteria extraction with the toxin concentration of 20  $\mu\text{g/mL}$  under irradiation by UV light (30 W). The  $t_{1/2}$  of MC degradation was 70~90 minutes. Photocatalysis has been shown to be more effective than photodegradation on MCs degradation. Shephard et al. [30] fixed a  $\text{TiO}_2$  catalyst on fiberglass to form a vertical film UV catalytic oxidation reactor. It was found that MC-LR and MC-RR degradations in deionized water were in agreement with first-order reaction kinetics. The  $t_{1/2}$  of the MC-LR and MC-RR degradation was 2.7 and 3.5 minutes, respectively, with rate constants of 0.255 and 0.199  $\text{min}^{-1}$ . Based on these results, it was verified that the efficiency of UV-micro $\text{O}_3$  process on MCs degradation is between photodegradation and photocatalysis.

**3.5. Effect of the Initial MCs Concentration on MCs Degradation.** Three different volumes of cyanobacteria extraction were mixed with 5 L deionized water. The MC concentrations were  $C_1$ ,  $C_2$ , and  $C_3$  from low to high (3.57, 6.72, and

12.75  $\mu\text{g/L}$  for MC-RR; 1.67, 3.12, and 6.02  $\mu\text{g/L}$  for MC-YR; and 1.54, 2.71, and 5.23  $\mu\text{g/L}$  for MC-LR). The MCs concentration in treated water and MCs removal efficiency of UV-micro $\text{O}_3$  process under different reaction times were summarized in Figure 7.

The results in Figure 7 showed that all of the MC degradation curves tend to be stable after a certain time, and concentrations of the same MC are nearly the same at the steady stage. The sample with the higher initial concentration needs longer time to reach stabilization. For each kind of MC, the removal rate and  $t_{1/2}$  are independent of initial concentration during the reaction process. The results further confirm that MC degradation by UV-micro $\text{O}_3$  process follows pseudofirst-order kinetics, which was in accordance with the results listed in Section 3.4.

**3.6. Effect of Organic Substance on MC Removal.** Equivalent amounts of cyanobacteria extractions were added to three water samples including deionized water, deionized water containing glucose, and the treated lake water (coagulation, sedimentation, and filtration). Static experiments were conducted with these three samples. The conventional process (coagulation, settlement, and filtration) cannot remove dissolved MCs effectively in lake water. Meanwhile, the surface water also contains natural organic matters (NOM). NOM mainly consists of humus and alga organic matter, which was the representative substance for  $\text{COD}_{\text{Mn}}$  and the main source of UV $_{254}$ . Glucose in deionized water can be easily degraded and would not absorb UV light. It was clear that organic materials in three water samples were significant to compare the influence of organic matter on MCs removal. The removal results were shown in Figure 8.

At the initial reaction stage, MC-RR of sample #1 revealed a slower degradation period which was about 20 minutes, compared to 10 minutes for MC-YR and MC-LR. The rates

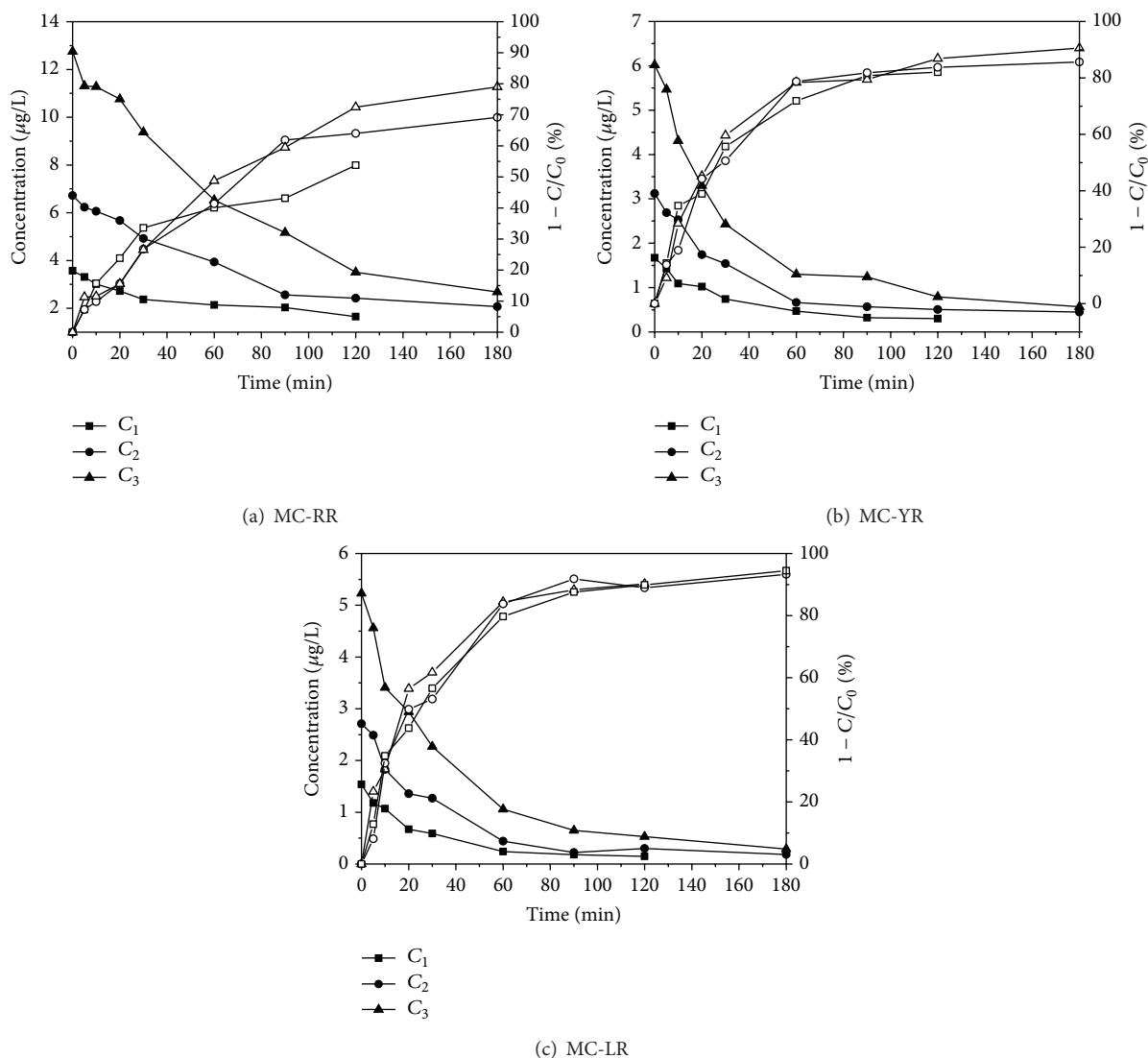


FIGURE 7: Comparison of MCs degradation at various initial concentrations.

of MC degradation were 29, 26, and 27 ng/(L·min) for MR-RR, MC-YR, and MC-LR, respectively. Subsequently, the degradation reaction came to a rapid period at reaction time beyond 20 min. Within 20 minutes, the average degradation rates of MC for three samples were 40, 47, and 58 ng/(L·min), respectively. The results showed that the NOM in lake water inhibits MCs degradation. The degradations of sample #2 and sample #3 were similar, without the slow degradation period at the initial reaction stage. The initial degradation rates of MCs in both sample #2 and sample #3 were 57 and 58 ng/(L·min), respectively, indicating that glucose has no effect on MCs degradation.

Any factors influencing UV absorption by MCs and radical hydroxyl production would have an effect on MCs degradation. NOM, such as pigments and humus in natural water, would accelerate the degradation of MCs [29] on photodegradation. On the other hand, NOM captures radical hydroxyls such as  $\cdot\text{OH}$  and consumes them to inhibit

the degradation of MCs. In UV-micro $\text{O}_3$  process, the MC degradation rate of sample #1 was lower than those of other water samples because of NOM present in treated lake water. This indicated that NOM's inhibition effect on MC degradation was stronger than NOM's promotion effect on photodegradation. The results also demonstrated that MC degradation was mainly through the oxidization of radical hydroxyls.

Four processes, UV- $\text{O}_3$ , UV-micro $\text{O}_3$ ,  $\text{O}_3$ , and micro $\text{O}_3$ , were further tested for the MCs degradation. The  $\text{O}_3$  concentrations in these four processes were 1.56, 0.76, 1.78, and 0.73 mg/L, respectively. The results showed that the  $t_{1/2}$  of MC-LR was 8.73, 24.3, 29.6, and 73.7 minutes, respectively. This illuminated that UV radiation and high ozone dose could accelerate the degradation of MCs.

Although UV- $\text{O}_3$  process showed the best degradation capability, the UV-micro $\text{O}_3$  process was still recommended as a suitable advanced treatment process for the degradation

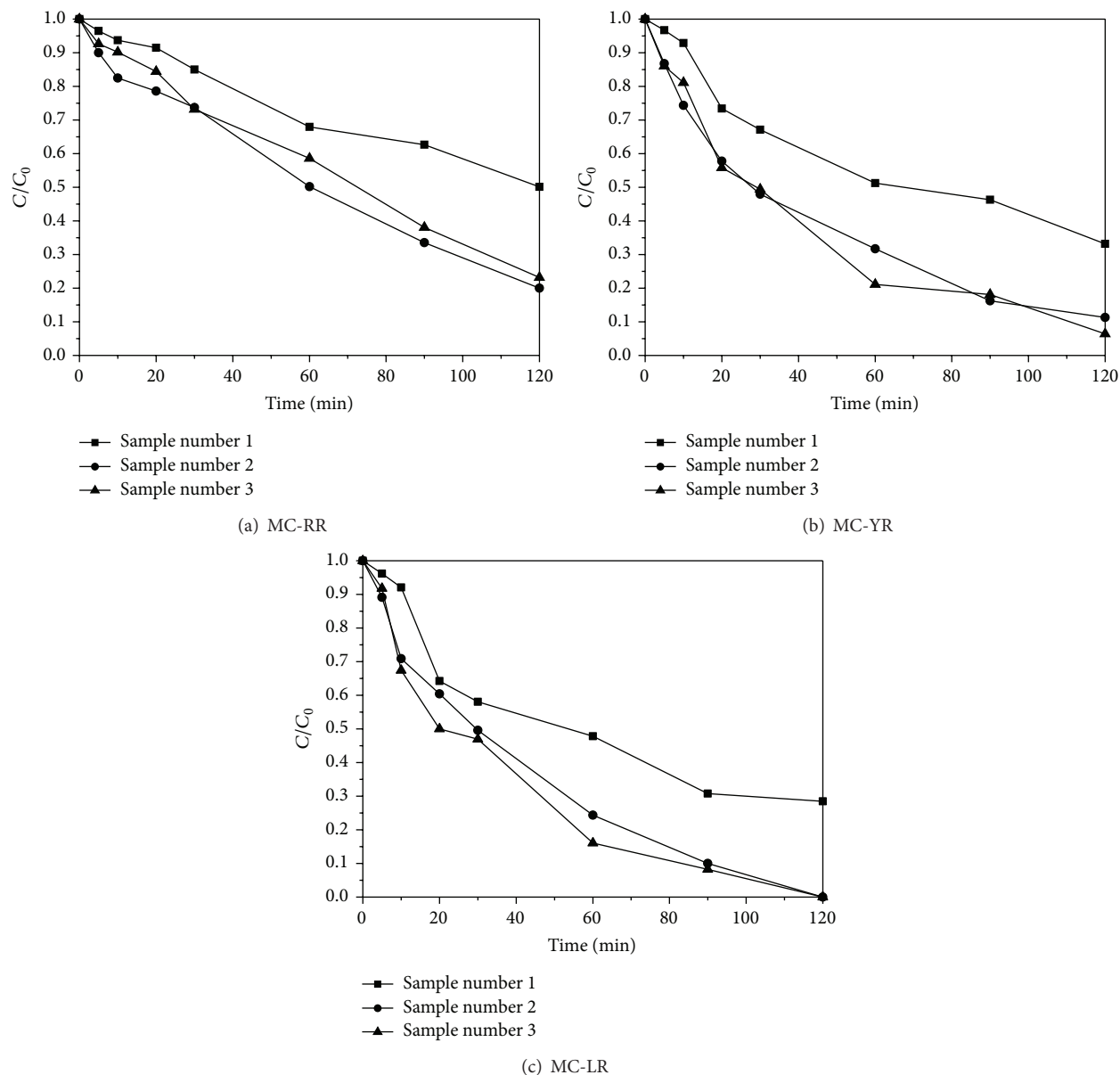


FIGURE 8: Effect of organic substances on the degradation of MCs.

of dissolved MCs due to both the degradation efficiency and expenses. When the HRT was more than 90 minutes, the MCs concentrations in finished water meet the sanitary standard for drinking water quality.

The reaction mechanism during UV-microO<sub>3</sub> process is summarized as follows [31]. Under the UV radiation, an organic molecule is decomposed directly and O<sub>2</sub> in the air is dissociated with small amounts of ozone generation. The air with microO<sub>3</sub> then disperses in water. With further activation by UV radiation, O<sub>3</sub> and dissolved oxygen are decomposed into <sup>•</sup>OH, O<sup>•</sup>, excited O<sub>2</sub>, and other species with strong oxidation potential. Moreover, the organic molecules are also activated by UV radiation and decompose by the interaction with <sup>•</sup>OH, O<sup>•</sup>, O<sub>3</sub>, and activated O<sub>2</sub>. MCs degradation in the UV-microO<sub>3</sub> process is not only by direct photolysis of UV,

but also by electron synthesis between the strong oxidative hydroxyl radicals and the unsaturated bonds of the Adda [30]. The destroyed Adda groups are separated from the ring structure of MCs and the toxicity disappears. At present, the exact degradation mechanism and products of MCs by UV-radiation and oxidation still need further investigation.

#### 4. Conclusions

The reactor equipped with 37 mm diameter quartz tube was selected. The optimum air flux was 18~25 L/h, and the O<sub>3</sub> concentration was 0.80~0.67 mg/L. In order to get the optimum ozone output, the air pressure and air humidity in the UV-microO<sub>3</sub> reactor should be as low as possible.

The UV-microO<sub>3</sub> process can degrade three kinds of MCs effectively. The MC degradation was characterized by first-order reaction kinetics. The pseudofirst-order kinetic constants for MC-RR, MC-YR, and MC-LR were 0.0093, 0.0215, and 0.0286 min<sup>-1</sup>, respectively.

The NOM in lake water can capture hydroxyl radicals and inhibit MC degradation. MCs in lake water treated by conventional processes first exhibited the slow degradation period and then converted to the rapid degradation period. Glucose had no influence on MCs degradation.

## Conflict of Interests

The authors declare that there is no conflict of interests regarding the publication of this paper.

## Acknowledgments

This work was financially supported by the National Major Special Technological Programmes Concerning Water Pollution Control and Management (no. 2014ZX07405002). The kind suggestions from the anonymous reviewers are also greatly acknowledged.

## References

- [1] J. L. Gong, Y. D. Liu, and X. B. Sun, "O<sub>3</sub> and UV/O<sub>3</sub> oxidation of organic constituents of biotreated municipal wastewater," *Water Research*, vol. 42, no. 4-5, pp. 1238–1244, 2008.
- [2] M. S. Lucas, J. A. Peres, and G. Li Puma, "Treatment of winery wastewater by ozone-based advanced oxidation processes (O<sub>3</sub>, O<sub>3</sub>/UV and O<sub>3</sub>/UV/H<sub>2</sub>O<sub>2</sub>) in a pilot-scale bubble column reactor and process economics," *Separation and Purification Technology*, vol. 72, no. 3, pp. 235–241, 2010.
- [3] E. J. Rosenfeldt, K. G. Linden, S. Canonica, and U. von Gunten, "Comparison of the efficiency of ·OH radical formation during ozonation and the advanced oxidation processes O<sub>3</sub>/H<sub>2</sub>O<sub>2</sub> and UV/H<sub>2</sub>O<sub>2</sub>," *Water Research*, vol. 40, no. 20, pp. 3695–3704, 2006.
- [4] H. Kusic, N. Koprivanac, and A. L. Bozic, "Minimization of organic pollutant content in aqueous solution by means of AOPs: UV-and ozone-based technologies," *Chemical Engineering Journal*, vol. 123, no. 3, pp. 127–137, 2006.
- [5] Y. F. Rao and W. Chu, "Degradation of linuron by UV, ozonation, and UV/O<sub>3</sub> processes—Effect of anions and reaction mechanism," *Journal of Hazardous Materials*, vol. 180, no. 1–3, pp. 514–523, 2010.
- [6] K. P. Wang, J. S. Guo, M. Yang, H. Junji, and R. Deng, "Decomposition of two haloacetic acids in water using UV radiation, ozone and advanced oxidation processes," *Journal of Hazardous Materials*, vol. 162, no. 2-3, pp. 1243–1248, 2009.
- [7] B. B. Xu, Z. L. Chen, F. Qi et al., "Inhibiting the regeneration of N-nitrosodimethylamine in drinking water by UV photolysis combined with ozonation," *Journal of Hazardous Materials*, vol. 168, pp. 108–114, 2009.
- [8] V. K. Gupta, "Application of low-cost adsorbents for dye removal—a review," *Journal of Environmental Management*, vol. 90, no. 8, pp. 2313–2342, 2009.
- [9] X. W. Lu, "Technology of drinking water treatment by ultraviolet/microozone process," Chinese patent, ZL96 117154.5. 2002-05-15.
- [10] G. Zhao, X. Lu, and Y. Zhou, "Aniline degradation in aqueous solution by UV-aeration and UV-microO<sub>3</sub> processes: efficiency, contribution of radicals and byproducts," *Chemical Engineering Journal*, vol. 229, pp. 436–443, 2013.
- [11] K. Kutschera, H. Börnick, and E. Worch, "Photoinitiated oxidation of geosmin and 2-methylisoborneol by irradiation with 254 nm and 185 nm UV light," *Water Research*, vol. 43, no. 8, pp. 2224–2232, 2009.
- [12] K. Zoschke, N. Dietrich, H. Börnick, and E. Worch, "UV-based advanced oxidation processes for the treatment of odour compounds: efficiency and by-product formation," *Water Research*, vol. 46, no. 16, pp. 5365–5373, 2012.
- [13] C. Svrcek and D. W. Smith, "Cyanobacteria toxins and the current state of knowledge on water treatment options: a review," *Journal of Environmental Engineering and Science*, vol. 3, no. 3, pp. 155–185, 2004.
- [14] W. W. Carmichael, "The toxins of cyanobacteria," *Scientific American*, vol. 270, no. 1, pp. 78–86, 1994.
- [15] M. R. Nishiwaki, T. Ohta, S. Nishiwaki et al., "Liver tumor promotion by the cyanobacterial cyclic peptide toxin microcystin-LR," *Journal of Cancer Research and Clinical Oncology*, vol. 118, no. 6, pp. 420–424, 1992.
- [16] V. K. K. Upadhyayula, S. Deng, M. C. Mitchell, and G. B. Smith, "Application of carbon nanotube technology for removal of contaminants in drinking water: a review," *Science of the Total Environment*, vol. 408, no. 1, pp. 1–13, 2009.
- [17] K. Tsuji, T. Watanuki, F. Kondo et al., "Stability of microcystins from cyanobacteria-II: effect of UV light on decomposition and isomerization," *Toxicon*, vol. 33, no. 12, pp. 1619–1631, 1995.
- [18] E. Rodríguez, G. D. Onstad, T. P. J. Kull, J. S. Metcalf, J. L. Acero, and U. von Gunten, "Oxidative elimination of cyanotoxins: comparison of ozone, chlorine, chlorine dioxide and permanganate," *Water Research*, vol. 41, no. 15, pp. 3381–3393, 2007.
- [19] J. Rositano, G. Newcombe, B. Nicholson, and P. Sztajnbock, "Ozonation of nom and algal toxins in four treated waters," *Water Research*, vol. 35, no. 1, pp. 23–32, 2001.
- [20] S. Brooke, G. Newcombe, B. Nicholson, and G. Klass, "Decrease in toxicity of microcystin LA and LR in drinking water by ozonation," *Toxicon*, vol. 48, no. 8, pp. 1054–1059, 2006.
- [21] F. Al Momani, "Degradation of cyanobacteria anatoxin-a by advanced oxidation processes," *Separation and Purification Technology*, vol. 57, no. 1, pp. 85–93, 2007.
- [22] J. Hart, J. K. Fawell, and B. Croll, "The fate of both intra- and extracellular toxins during drinking water treatment," in *Proceedings of the IWSA World Congress*, Special Subject no. 18, SS18-1-6, Madrid, Spain, September 1997.
- [23] H. Miao and W. Tao, "The mechanisms of ozonation on cyanobacteria and its toxins removal," *Separation and Purification Technology*, vol. 66, no. 1, pp. 187–193, 2009.
- [24] X. Liu, Z. Chen, N. Zhou, J. Shen, and M. Ye, "Degradation and detoxification of microcystin-LR in drinking water by sequential use of UV and ozone," *Journal of Environmental Sciences*, vol. 22, no. 12, pp. 1897–1902, 2010.
- [25] X. He, M. Pelaez, J. A. Westrick et al., "Efficient removal of microcystin-LR by UV-C/H<sub>2</sub>O<sub>2</sub> in synthetic and natural water samples," *Water Research*, vol. 46, no. 5, pp. 1501–1510, 2012.

- [26] A. Latifoglu and M. D. Gurol, "The effect of humic acids on nitrobenzene oxidation by ozonation and  $O_3$ /UV processes," *Water Research*, vol. 37, no. 8, pp. 1879–1889, 2003.
- [27] J. Wenk, U. von Gunten, and S. Canonica, "Effect of dissolved organic matter on the transformation of contaminants induced by excited triplet states and the hydroxyl radical," *Environmental Science and Technology*, vol. 45, no. 4, pp. 1334–1340, 2011.
- [28] L. A. Lawton, P. K. J. Robertson, B. J. P. A. Cornish, and M. Jaspars, "Detoxification of microcystins (cyanobacterial hepatotoxins) using  $TiO_2$  photocatalytic oxidation," *Environmental Science and Technology*, vol. 33, no. 5, pp. 771–775, 1999.
- [29] W. H. Zhang, T. Fang, and X. Q. Xu, "Study on photodegradation of cyanobacterial toxin in blooms of Dianchi Lake," *China Environmental Science*, vol. 21, no. 1, pp. 1–3, 2001 (Chinese).
- [30] G. S. Shephard, S. Stockenström, D. De Villiers, W. J. Engelbrecht, and G. F. S. Wessels, "Degradation of microcystin toxins in a falling film photocatalytic reactor with immobilized titanium dioxide catalyst," *Water Research*, vol. 36, no. 1, pp. 140–146, 2002.
- [31] Q. C. Kong, *Study on the Degradation of Microorganic Priority Pollutants by UV-Micro $O_3$  Oxidation Process*, College of Civil Engineering, Southeast University, Nanjing, China, 1995, (Chinese).



**Hindawi**

Submit your manuscripts at  
<http://www.hindawi.com>

